ACS APPLIED MATERIALS & INTERFACES

Research Article

www.acsami.org

High-Performance Large-Scale Flexible Dye-Sensitized Solar Cells Based on Anodic TiO_2 Nanotube Arrays

Hsiu-Ping Jen,[†] Meng-Hung Lin,[†] Lu-Lin Li,[†] Hui-Ping Wu,[†] Wei-Kai Huang,[†] Po-Jen Cheng,[‡] and Eric Wei-Guang Diau*[,†]

[†]Department of Applied Chemistry and Institute of Molecular Science, National Chiao Tung University, Hsinchu 30010, Taiwan

[‡]Niching Industrial Crop. Room 5E, No.97, Sec. 3, Taijunggang Road, Taichung 400, Taiwan

Supporting Information

ABSTRACT: A simple strategy to fabricate flexible dye-sensitized solar cells involves the use of photoanodes based on TiO_2 nanotube (TNT) arrays with rear illumination. The TNT films (tube length ~35 μm) were produced via anodization, and sensitized with N719 dye for photovoltaic characterization. Pt counter electrodes of two types were used: a conventional FTO/glass substrate for a device of rigid type and an ITO/PEN substrate for a device of flexible type. These DSSC devices were fabricated into either a single-cell structure (active area 3.6 × 0.5 cm^2) or a parallel module containing three single cells (total active area 5.4 cm^2). The flexible devices exhibit remarkable performance with efficiencies η = 5.40 % (single cell) and 4.77 % (parallel module) of power conversion, which outperformed their rigid counterparts with η = 4.87 % (single cell) and 4.50 % (parallel model) under standard one-sun irradiation. The flexible device had a greater efficiency of conversion of incident photons to current and a broader spectral range than the rigid device; a thinner electrolyte layer for the flexible device than for the rigid device is a key factor to improve the light-harvesting ability for the TNT-DSSC device with rear illumination. Measurements of electrochemical impedance spectra show excellent catalytic activity and superior diffusion characteristics for the flexible device. This technique thus provides a new option to construct flexible photovoltaic devices with large-scale, light-weight, and cost-effective advantages for imminent applications in consumer electronics.

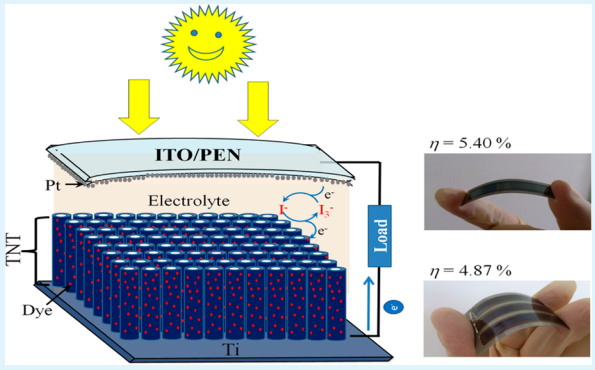

KEYWORDS: *anodization, DSSC, EIS, flexible optoelectronics, TiO_2 nanotubes*

INTRODUCTION

Dye-sensitized solar cells (DSSC) attract attention because of their potential as next-generation photovoltaic devices.[1] The efficiency of power conversion of a porphyrin-based DSSC using a traditional glass-based TiO_2 photoanode has exceeded 12.3 %.[2] For prospective applications of DSSC, flexibility is important, because such electronics have the advantages of low cost, light weight and thin structure, and they are bendable, portable, convenient, and easily processed. Many researchers have hence focused on the development of flexible DSSC.[3−10] The challenge in making flexible DSSC, relative to traditional glass-type rigid DSSC, is to enhance the connectivity of TiO_2 nanoparticles (NP) on a conducting plastic substrate at a temperature <150 °C because a plastic substrate is easily damaged or subject to thermal destruction during a required sintering of TiO_2 > 450 °C. To overcome this problem, many processes at low temperature have been developed,[11−14] but they produce poorly crystalline and vulnerable component materials, limiting their applications for flexible DSSC. The efficiencies of the plastic-made flexible DSSC were accordingly less than those of glass-made rigid DSSC using TiO_2 NP as photoanode material.[15−17] To improve the cell performance from a plastic-made DSSC, we applied one-dimensional TiO_2 nanotube (TNT) arrays as potential photoanode materials to fabricate large-scale flexible DSSC,[18−21] because they have superior electron transport and their rate of charge recombination is smaller than that of a conventional NP-based system.[22]

We developed a hybrid anodization method in two steps, first potentiostatic anodization and then galvanostatic anodization, to grow long, ordered arrays of TNT in a short anodization period.[23] As a consequence, the cell performance of a NT-DSSC with tube length ~30 μm was optimized to attain 7.6 % for a structure with rear illumination. Because the TNT arrays are grown on thin and highly flexible Ti foil, the TNT photoanode becomes a suitable candidate for use in a flexible DSSC device. Here we report high-performance flexible NT-DSSC of two types: (1) a single cell of active area 3.6 × 0.5 =

Received: July 6, 2013
Accepted: September 20, 2013
Published: September 20, 2013

Scheme 1. Schematic Diagram of Fabrication of NT-DSSC Devices of Two Types − Flexible (ITO/PEN) and Rigid (FTO/glass)

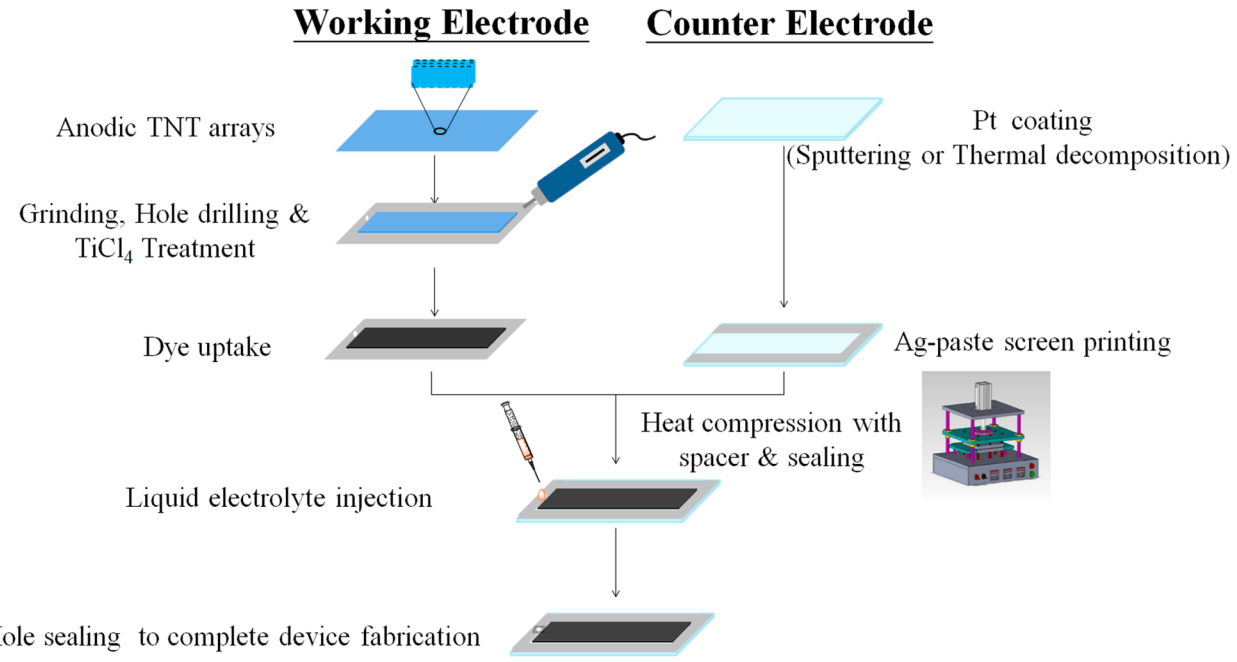

1.8 cm^2, and (2) a parallel module containing three single cells of the same size in a parallel circuit of total light-active area 5.4 cm^2. Pt counter electrodes (CE) of two types are applied: (1) an ITO/PEN substrate to make flexible devices and (2) a FTO/glass substrate to make their rigid counterparts for comparison. For the flexible single cell, we obtained J_{SC} = 12.49 mA cm^{-2}, V_{OC} = 0.708 V, FF = 0.61, and η = 5.40 %; for the flexible parallel module, J_{SC} = 12.86 mA cm^{-2}, V_{OC} = 0.728 V, FF = 0.51, and η = 4.77 %; both flexible devices with a thinner layer of electrolyte are superior to their rigid counterparts. To understand the performance discrepancy between the flexible and the rigid devices, we measured the efficiency of conversion of incident photons to current (IPCE) and electrochemical impedance spectra (EIS).

EXPERIMENTS

Synthesis of TiO_2 NT Arrays. The titanium-dioxide nanotube arrays were fabricated with a standard anodization method reported elsewhere.[19,23−25] Ti foil (commercially pure grade 1, purity 99.9 %, substrate size 6 × 6 cm^2, thickness 130 μm, Kobe Steel) served as anode on which to grow TNT arrays with another Ti foil of the same size as cathode. The ordered TNT films were produced in electrolyte solutions containing NH_4F (purity 99.9 %, 0.4 mass %) in ethandiol in the presence of H_2O (2 vol %) at 60 V for 8 h at 25 °C. The sample as anodized was washed in ethanol, and annealed at 450 °C for 1 h to convert the amorphous TiO_2 to an anatase crystalline phase.[23−26] To remove the debris on the tube surfaces, we treated the sample with ultrasonic agitation in ethanol for 15 min.

$TiCl_4$ Post-treatment. The NT films were treated with $TiCl_4$ in two stages.[19] The films as prepared were first immersed in $TiCl_4$ solution (0.073 M) for 30 min followed by rinsing and drying near 56 °C. The films were re-immersed in $TiCl_4$ stock solution for 2 h and annealed at 350 °C for 30 min. The effect of $TiCl_4$ post-treatment on TNT films can be understood to form a densely packed TiO_2 NP layer on the surface of the tubes, which enhanced the amounts of dye-loading as we have previously demonstrated.[19]

Fabrication of the Flexible and Rigid DSSCs Based on TNT Arrays. We immersed the TNT films (single, 3.6 × 0.5 cm^2; parallel, 3 × 3.6 × 0.5 cm^2) in a solution of N719 dye (3×10^{-4} M, Solaronix) containing chenodeoxycholic acid (CDCA, 3×10^{-4} M) in acetonitrile/tert-butanol (v/v = 1/1) binary solvent for 18 h to absorb sufficient N719 dye for light harvesting. The samples were then washed with ethanol to remove the remaining dye. In the fabrication of a NT-DSSC device, the N719/TNT film served as an anode combined with a transparent Pt counter electrode as a cathode. Cathodes of two types were used. For the flexible and rigid DSSCs, Pt was sputtered onto a substrate of indium tin oxide/polyethylene naphthalate (ITO/PEN; 13 Ω/sq, PECF-IP, Peccell, Japan) plastic and a fluorine-doped tin-oxide (FTO; 7 Ω/sq)/glass (TEC 7, Hartford, USA) for about 10 s, respectively. Furthermore, for rigid DSSC, a H_2PtCl_6 /isopropanol solution was also used spin-coated onto a FTO substrate through thermal decomposition at 385 °C for 15 min. To enhance the electric conductivity, we coated the edges of all Pt counter electrodes with a layer of silver in a Ag-gel paste through screen printing. The NT-DSSC devices were simply sealed with a hot-molten film (SX1170, Solaronix, thickness 60 μm); electrolyte was introduced as a thin layer into the space between the two electrodes. A typical electrolyte contained lithium iodide (LiI, 0.1 M), diiodine (I_2, 0.01 M), 4-tert-butylpyridine (TBP, 0.5 M), butylmethyl- imidazolium iodide (BMII, 0.6 M), and guanidinium thiocyanate (GuNCS, 0.1 M) in a 3-methoxypropionitrile (MPN). The detailed fabrication procedure is summarized in Scheme 1.

Current−Voltage Characteristics. The current−voltage characteristics were measured with a digital source meter (Keithley 2400, computer-controlled) with the device under standard AM-1.5G one-sun irradiation from a solar simulator (XES-40S1, SAN-EI) calibrated with a standard silicon reference cell (VLSI standards, Oriel PN 91150 V). The

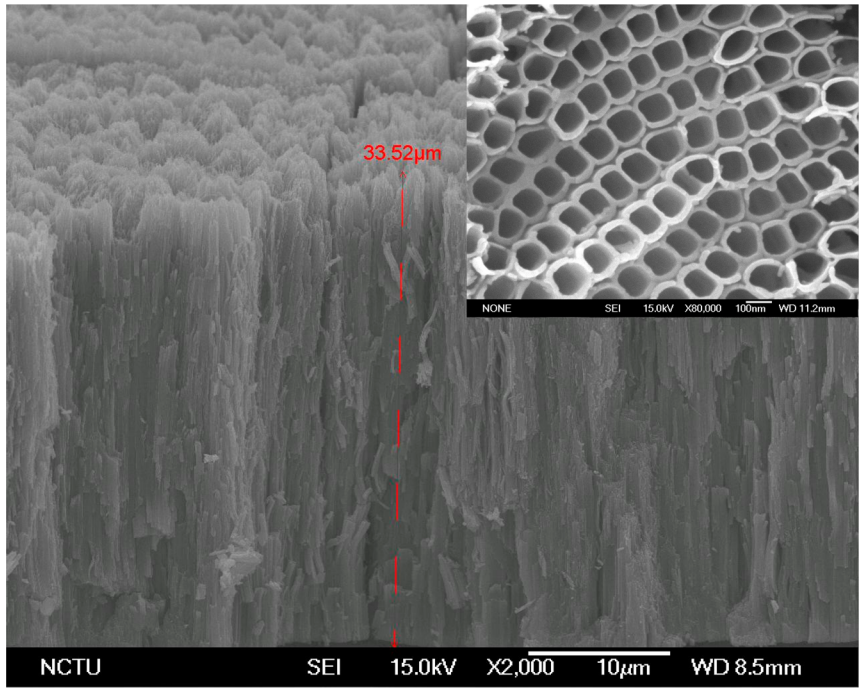

Figure 1. Side-view image (scanning electron microscope, SEM) of the TNT film utilized as photoanode for flexible and rigid NT-DSSC devices. The inset shows the SEM top-view image of the corresponding TNT arrays.

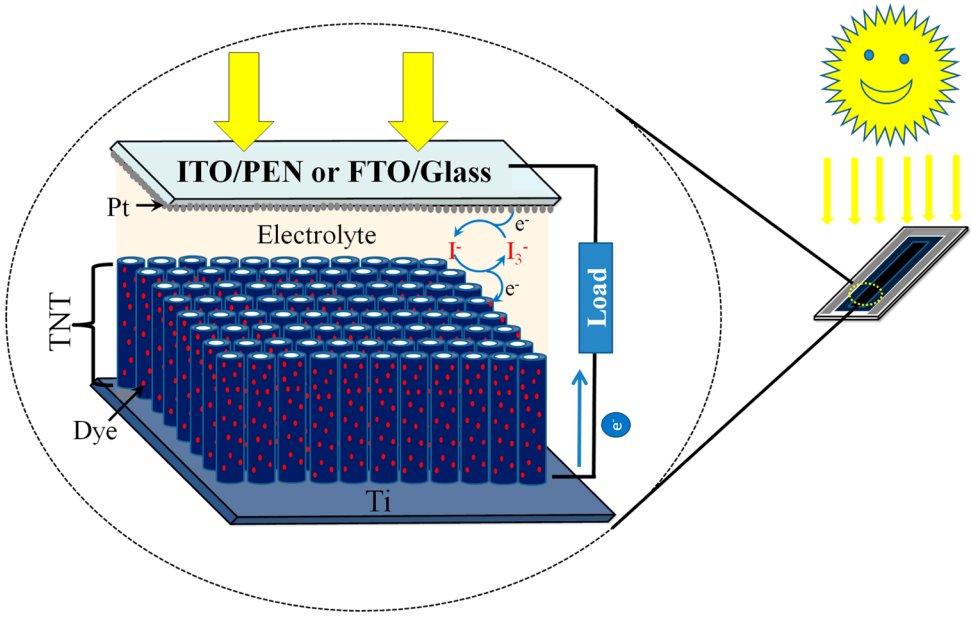

Figure 2. Schematic diagram of the composition for a NT-DSSC device under rear illumination.

efficiency (η) of power conversion was obtained via $\eta = J_{SC}V_{OC}FF/P_{in}$, in which J_{SC} (mA cm^{-2}) is the current density measured at short circuit, and V_{OC} (V) is the voltage measured at open circuit. P_{in} is the input radiation power (for one-sun illumination P_{in} = 100 mW cm^{-2}) and FF is the fill factor.

Measurements of Electrochemical Impedance Spectroscopy (EIS). To determine the electron transport properties of the DSSC devices, we measured electrochemical impedance spectra (EIS) using an impedance characterization unit (IM6, Zahner) in a two-electrode design; the TNT array film served as a working electrode and the Pt-coated ITO/PEN or FTO/glass as a counter electrode at an applied bias of the open circuit voltage under one-sun irradiation. The frequency range was 50 mHz to 1 MHz; the magnitude of the alternating potential was 20 mV. The EIS data were analyzed with an appropriate equivalent circuit using simulation software (Zahner).

Measurements of Incident Photon-to-Current Conversion Efficiency (IPCE). The spectra of the efficiency of conversion of incident photons to current (IPCE) of the corresponding devices were obtained with a photoelectric spectral system[19] containing a Xe lamp (PTi A-1010, 150 W), a monochromator (PTi, 1200 gr mm^{-1} blazed at 500 nm), and a source meter (Keithley 2400).

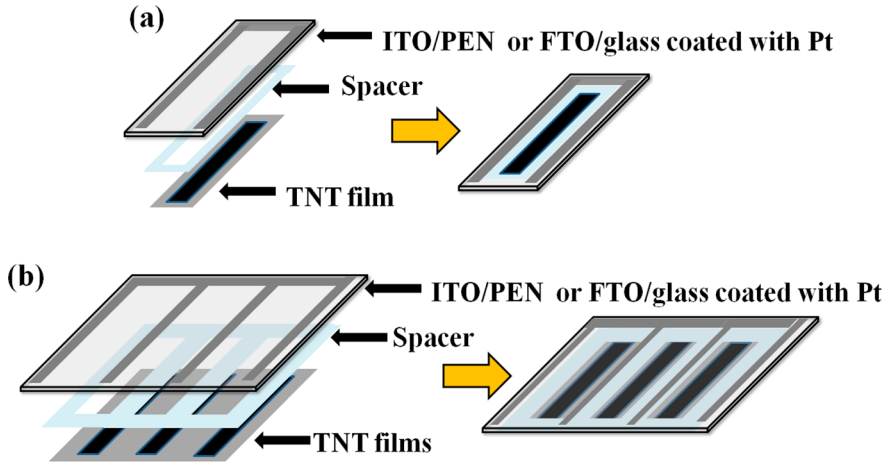

Figure 3. Schematic representation of fabrication of a flexible (ITO/PEN) or a rigid (FTO/glass) NT-DSSC device for (a) single cell (active area 0.5 × 3.6 = 1.8 cm^2) and (b) parallel module (active area 3 × (0.5 × 3.6) = 5.4 cm^2).

RESULTS AND DISCUSSION

The advantage of TNT arrays to replace TiO_2 NP for DSSC is the one-dimensional structural feature of TNT such that electron transport is more efficient through TNT than through NP.[22] For recently developed TNT-based DSSC, the performance of the corresponding NT-DSSC has increased to η = 7.6 % based on a photoanode made of TNT arrays of tube length 30 μm and a Pt-CE made of a FTO/glass substrate of active area 0.5 × 0.5 cm^2.[23] Because of the flexible nature of the TNT films, in the present work we fabricated NT-DSSC of large-scale flexible type using the Pt-CE made of an ITO/PEN substrate. Figure 1 shows a SEM image of a typical TNT array with tube length (L) = 33.5 μm. The nanotubes possess a hollow conical columnar structure;[25] according to the top-view SEM image shown in the inset of Figure 1, the average pore diameter on the top of the film is ~100 nm. Figure 2 shows the cell structure of our NT-DSSC device. NT-DSSC devices of two types were fabricated: the flexible type had an ITO/PEN plastic as Pt-CE, whereas the rigid type had a FTO/glass substrate as Pt-CE. We designed the NT-DSSC device shaped as a long strip for the size of the TNT film fixed at 0.5 cm in width and 3.6 cm in length (light-active area =1.8 cm^2). To extend the availability of NT-DSSC for future applications, we combined three single cells of the same size to form a parallel module of light-active area 5.4 cm^2. Figures 3a and 3b show the device configurations for the NT-DSSC devices of a single cell and a parallel module, respectively.

To compare the photovoltaic performance of the flexible and rigid NT-DSSC devices (single cells), we fabricated the Pt counter electrodes using different methods to obtain the optimized device performance. Both thermal decomposition and sputtering methods were used for rigid DSSCs, but only sputtering method was applied for flexible devices due to the problem of thermal stability for the plastic substrates. Figures S1 and S2 in the Supporting Information show the device performances of the rigid DSSC with the Pt counter electrodes made of the thermal decomposition and sputtering methods, respectively. Because the overall device performances of the former were significantly greater than the latter, the Pt counter electrodes of the rigid NT-DSSC devices were made by the thermal decomposition method rather than by the sputtering method that we must apply to fabricate the flexible devices.

Panels a and b in Figure 4 show the current–voltage characteristic and IPCE action spectra, respectively. For the

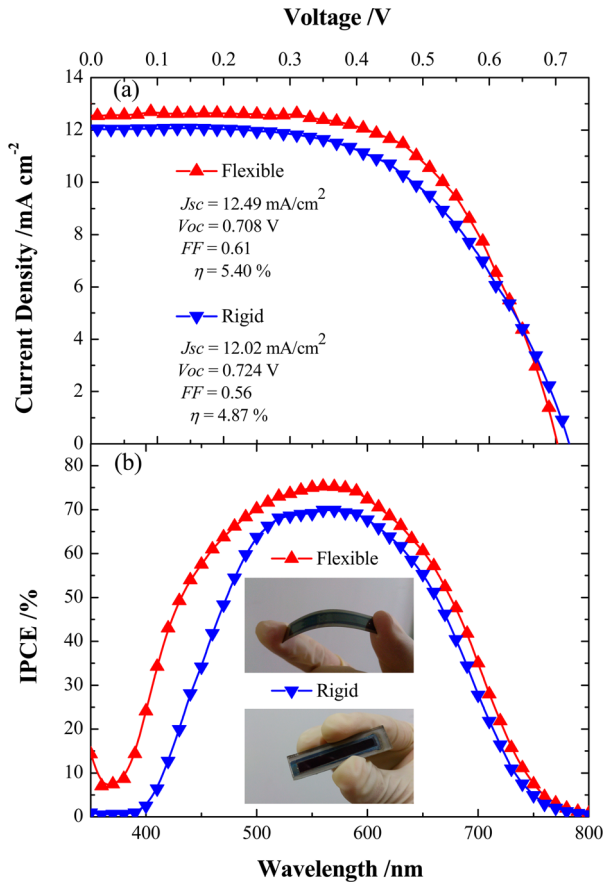

Figure 4. (a) Current–voltage characteristics and (b) IPCE action spectra of flexible and rigid NT-DSSC devices (single cells of active area 1.8 cm^2). Flexible (▲) and rigid (▼).

flexible single cell, we obtained J_{SC} = 12.49 mA cm^{-2}, V_{OC} = 0.708 V, FF = 0.61, and overall power conversion efficiency η = 5.40 %; for the rigid counterpart, we obtained J_{SC} = 12.02 mA cm^{-2}, V_{OC} = 0.724 V, FF = 0.56, and η = 4.87 %. J_{SC} of the flexible cell evidently exceeds that of its rigid counterpart, yielding superior performance of the flexible device over that of

the rigid device. The detailed photovoltaic parameters are presented in Table 1. The IPCE property shown in Figure 4b

Table 1. Photovoltaic Performances of DSSC Based on Anodic TiO_2 Nanotube Arrays[a]

device	counter electrode	J_{SC} (mA cm^{-2})	V_{OC} (V)	FF	η (%)
single cell	flexible	12.49	0.708	0.61	5.40
	rigid	12.02	0.724	0.56	4.87
parallel module	flexible	12.86	0.728	0.51	4.77
	rigid	11.32	0.764	0.52	4.50

[a]The photoelectrodes have thickness ~35 μm and active areas 1.8 cm^2 (single) and 5.4 cm^2 (parallel).

indicates further that the action spectrum of the flexible cell is broader with greater efficiencies than those of the rigid device. The native drawback of a NT-DSSC device is known to be its rear-illumination structure, which has limited the performance for harvesting of radiation from the CE side; a smaller J_{SC} was hence obtained from a NT-DSSC than from a conventional front-illuminated NP-based DSSC. The loss of incident light in the rear-illuminated NT-DSSC was caused mainly from the reflection of the Pt-CE and the absorption of the iodide/triiodide electrolyte. Although both rigid and flexible devices were fabricated using the same hot-melt film (thickness 60 μm) as a spacer to separate the two electrodes, the distance between the two electrodes is expected to be smaller in the flexible device than in the rigid one because of the spacing flexibility for the device with two flexible electrodes. Our IPCE results clearly show this advantage for the flexible device with a thinner layer of electrolyte, making the loss much less than for the rigid one. This thin-layer property is a key factor to improve the light-harvesting ability for the NT-DSSC devices with rear illumination. The flexible plastic Pt-CE to fabricate a flexible NT-DSSC is beneficial because of a thin layer of electrolyte for improved light harvesting; concurrently the one-dimensional nanostructure of the TNT arrays with its superior charge-collection efficiency[22] is beneficial to obtain an excellent device performance for a long strip flexible device with large active area.

Figure 5 shows the photovoltaic performances for comparison with the parallel NT-DSSC modules (active area 5.4 cm^2) between the flexible and the rigid devices; the corresponding photovoltaic parameters are shown in Table 1. For the flexible module, we obtained J_{SC} = 12.86 mA cm^{-2}, V_{OC} = 0.728 V, FF = 0.51, and overall power- conversion efficiency η = 4.77 %; for its rigid counterpart, we obtained J_{SC} = 11.32 mA cm^{-2}, V_{OC} = 0.764 V, FF = 0.52, and η = 4.50 %. The flexible module has J_{SC} greater than that of the rigid counterpart for the same reason as for the single cells, improving the performance of the flexible module over that of the rigid module. Both J_{SC} and V_{OC} of the three-cell modules were comparable to those of the single cells, but FF was substantially smaller for the modules than for the cells. To understand the factors governing the device performance, we investigated the interfacial resistances using EIS.

To investigate the internal problems of the devices, we measured EIS under one-sun irradiation; the results appear in Figure 6 with the relevant EIS parameters summarized in Table 2. Figure 6a depicts the equivalent circuit model for our work; R_s denotes the series resistance, R_{tr} the electron-transport resistance in the TiO_2 matrix, R_{rec} the charge-transfer resistance

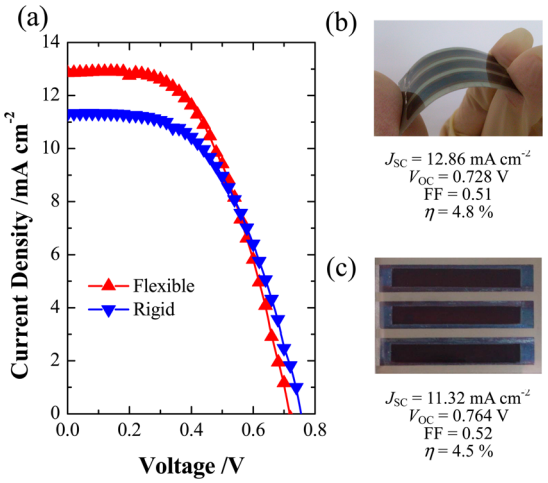

Figure 5. (a) Current–voltage characteristics of flexible and rigid NT-DSSC devices (parallel modules of active area 5.4 cm^2). (b, c) Pictures of the devices and the corresponding photovoltaic performances of flexible and rigid modules, respectively.

related to recombination, R_d the diffusion resistance of redox species in the electrolyte, and R_{CE} is the charge-transfer resistance at the interface between counter electrode and electrolyte.[27] Figure 6b shows Nyquist plots for the same flexible and rigid single-cell devices with the corresponding photovoltaic performances shown in Figure 4. The EIS data were fitted according to an equivalent circuit model in Figure 6a; the fitted results are displayed as solid curves in Figure 6b.

Basically two semicircles are featured in the Nyquist plots of both cells. The onsets of the plots show series resistances (R_s = 2.5 Ω cm^2 for flexible devices and 1.9 Ω cm^2 for rigid) of both Ti and counter electrodes; the flexible ITO/PEN substrate has a larger sheet resistance than the rigid FTO/glass substrate. The semicircles in the high-frequency region represent the charge-transfer resistance: R_{CE} = 2.6 Ω cm^2 for the flexible NT-DSSC device and 5.0 Ω cm^2 for the rigid device. The smaller R_{CE} of the flexible cell indicates a performance of the platinized counter electrode for tri-iodide reduction better than that of the rigid cell, which might be due to different deposition methods employed to fabricate the counter electrodes. Because the plastic ITO/PEN substrates have poor thermal stability, platinum was deposited by sputtering instead of thermal reduction. The sputtering-coating method yields platinum nanoparticles of small size and uniform distribution deposited on the substrate producing a great electrocatalytic activity with a small R_{CE}. In the medium-frequency region of the Nyquist plots, the recombination resistances R_{rec} (Ω cm^2) at the TiO_2/electrolyte interface are 5.1 and 4.6 for flexible and rigid NT-DSSC devices, respectively. These similar values of the two devices indicate a common charge-recombination behavior as the same TNT arrays and electrolyte were used in both NT-DSSC devices. The resistances, R_d (Ω cm^2), because of diffusion in the electrolyte at the lowest frequencies show an apparent difference (3.2 vs. 4.8) between flexible and rigid devices, because the flexible device has a thinner layer of electrolyte than the rigid device. This result is consistent with the observed cell performance as greater J_{SC} and IPCE (also broader) were observed for the flexible than for the rigid device (Figure 4).

We tested the durability of the photovoltaic performance of the flexible TNT-based single cell (active area 1.8 cm^2) near 23

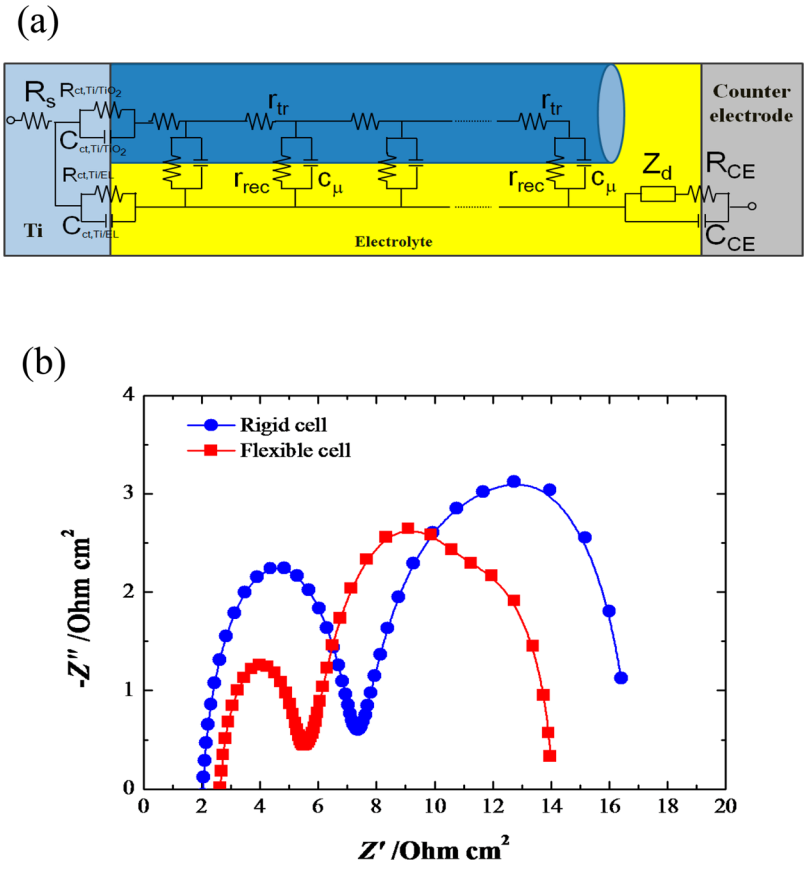

Figure 6. (a) Plot of equivalent circuit for the simulation of impedance spectra of NT-DSSC. (b) Nyquist plots obtained from electrochemical impedance spectra (EIS) for flexible (squares) and rigid (circles) NT-DSSC devices (active area 1.8 cm^2). Symbols represent the measured data and curves represent the fitted results according to the model shown in a.

Table 2. Fitted Parameters of Electrochemical Impedance Spectra (EIS) of DSSC Based on Anodic TiO_2 Nanotube Arrays[a]

counter electrode	R_s (Ω cm^2)	R_{CE} (Ω cm^2)	R_{tr} (Ω cm^2)	R_{rec} (Ω cm^2)	R_d (Ω cm^2)
flexible	2.5	2.6	1.7	5.1	3.2
rigid	1.9	5.0	1.2	4.6	4.8

[a]The photoelectrodes have thickness ~35 μm and active area 1.8 cm^2.

°C over 130 days. The cell efficiency was measured after storing it in the dark at room temperature. The photovoltaic parameters as a function of duration for this stability test are shown in Figure 7. The efficiency of the flexible device decreased from η = 5.0 % to 4.6 % in the first ten days, but the device performance became stabilized afterwards. The variation of J_{SC} shows a similar trend, but both V_{OC} and *FF* increased slightly at the beginning and then remained constant. After 130 days, the flexible NT-DSSC retained 90 % of the original efficiency of energy conversion.

CONCLUSIONS

Even though the best performance of a DSSC has attained the overall efficiency over 12 %,[2] fabrication of a large-scale device with excellent durability and flexibility is still a big industrial challenge because the TiO_2 photoanode in a traditional device requires a thermal treatment at a high temperature that impedes the development of a flexible DSSC using the conventional approach.[1,2] In the present study, we report a

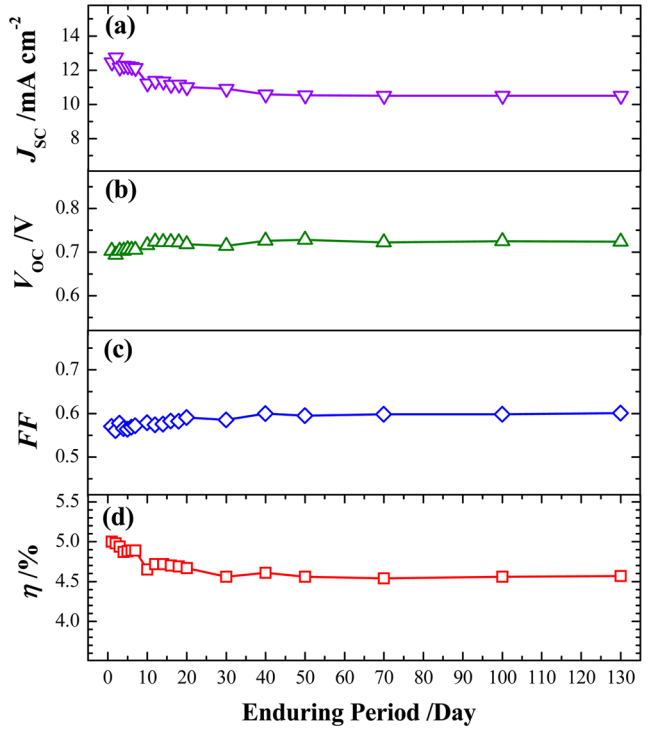

Figure 7. Evaluation of stability over 130 days for a single flexible cell (active area 1.8 cm^2) near 23 °C: (a) J_{sc}, (b) V_{oc}, (c) FF, and (d) η.

strategy to overcome this problem via fabrication of large-scale and highly efficient flexible DSSC devices with photoanodes composed of one-dimensional, vertically oriented, TNT arrays of tube length ~35 μm. Devices of two types were constructed for comparison: the flexible type used ITO/PEN whereas the rigid type used FTO/glass as substrate material for platinum counter electrodes. The NT-DSSC devices were optimized to attain efficiencies 5.40 % (flexible) and 4.87 % (rigid) of power conversion for single cells (active area 1.8 cm^2), and 4.77 % (flexible) and 4.50 % (rigid) for parallel modules comprised of three identical cells (active area 5.4 cm^2) under standard AM-1.5G one-sun irradiation. According to our IPCE and EIS characterizations, the devices of flexible type present a greater and broader light-harvesting spectral feature with superior catalytic activity and electrolyte diffusion characteristics because the flexible devices have a thinner layer of electrolyte than the rigid devices. The stability test indicates that the flexible NT-DSSC possessed great and durable performance near 23 °C suitable for indoor applications of future consumer electronics.

■ ASSOCIATED CONTENT

Supporting Information

Photocurrent−voltage (J−V) curves of the rigid DSSC with the Pt counter electrodes made of the thermal decomposition and sputtering methods. This material is available free of charge via the internet at http://pubs.acs.org.

■ AUTHOR INFORMATION

Corresponding Author

*E-mail: diau@mail.nctu.edu.tw..

Notes

The authors declare no competing financial interest.

■ ACKNOWLEDGMENTS

We thank Jonathan Chang, president of Niching Industrial Corporation, for his support of this project. National Science Council of Taiwan and Ministry of Education of Taiwan, under the ATU program, also provided financial support for this project.

■ REFERENCES

(1) Hagfeldt, A.; Boschloo, G.; Sun, L.; Kloo, L.; Pettersson, H. *Chem. Rev.* **2010**, *110*, 6595−6663.
(2) Yella, A.; Lee, H.-W.; Tsao, H. N.; Yi, C.; Chandiran, A. K.; Nazeeruddin, M. K.; Diau, E. W. -G.; Yeh, C.-Y.; Zakeeruddin, S. M.; Grätzel, M. *Science* **2011**, *334*, 629−634.
(3) Ito, S.; Ha, N. C.; Rothenberger, G.; Liska, P.; Comte, P.; Zakeeruddin, S. M.; Péchy, P.; Nazeeruddin, M. K.; Gärtzel, M. *Chem. Commun.* **2006**, 4004−4006.
(4) Yang, L.; Wu, L.; Wu, M.; Xin, G.; Lin, H.; Ma, T. *Electrochem. Commun.* **2010**, *12*, 1000−1003.
(5) Yamaguchi, T.; Tobe, N.; Matsumoto, D.; Nagai, T.; Arakawa, H. *Sol.Energy Mater. Sol.Cells* **2010**, *94*, 812−816.
(6) Lee, C.-H.; Chiu, W.-H.; Lee, K.-M.; Hsieh, W.-F.; Wu, J.-M. *J. Mater. Chem.* **2011**, *21*, 5114−5119.
(7) Chen, H.-W.; Liao, Y. -T.; Chen, J.-G.; Wu, C.-W.; Ho, K.-C. *J. Mater. Chem.* **2011**, *21*, 17511−17518.
(8) Chiua, W.-H.; Lee, K.-M.; Hsieh, W.-F. *J. Power Sources* **2011**, *196*, 3683−3687.
(9) Cha, S. I.; Kim, Y.; Hwang, K. H.; Shin, Y. J.; Seo, S. H.; Lee, D. Y. *Energy Environ. Sci.* **2012**, *5*, 6071−6075.
(10) Li, Y.; Lee, D. K.; Kim, J. Y.; Kim, B.; Park, N. G; Kim, K.; Shin, J. H.; Choi, I. S.; Ko, M. J. *Energy Environ. Sci.* **2012**, *5*, 8950−8957.
(11) Park, N. G.; Kim, K. M.; Kang, M. G.; Ryu, K. S.; Chang, S. H.; Shin, Y. J. *Adv. Mater.* **2005**, *17*, 2349−2353.
(12) Li, X.; Lin, H.; Li, J.; Wang, N.; Lin, C.; Zhang, L. *J. Photochem. Photobiol., A* **2008**, *195*, 247−253.
(13) Li, Y.; Lee, W.; Lee, D. K.; Kim, K.; Park, N. G.; Ko, M. J. *Appl. Phys. Lett.* **2011**, *98*, 103301−103304.
(14) Yamaguchi, T.; Tobe, N.; Matsumoto, D.; Arakawa, H. *Chem. Commun.* **2007**, 4767−4769.
(15) Kanga, M. G.; Park, N. G.; Ryu, K. S.; Chang, S. H.; Kim, K. J. *Sol. Energy Mater. Sol. Cells* **2006**, *90*, 574−581.
(16) Park, J. H.; Jun, Y.; Yun, H. G.; Lee, S. Y.; Kang, M. G. *J. Electrochem. Soc.* **2008**, *155*, F145−F149.
(17) Fan, K.; Gong, C.; Peng, T.; Chen, J.; Xia, J. *Nanoscale* **2011**, *3*, 3900−3906.
(18) Mor, G. K.; Shankar, K.; Paulose, M.; Varghese, O. K.; Grimes, C. A. *Nano Lett.* **2006**, *6*, 215−218.
(19) Chen, C.-C.; Chung, H.-W.; Chen, C.-H.; Lu, H.-P.; Lan, C.-M.; Chen, S.-F.; Luo, L.; Hung, C.-S.; Diau, E. W.-G. *J. Phys. Chem. C* **2008**, *112*, 19151−19157.
(20) Luo, L.; Lin, C.-J.; Tsai, C.-Y.; Wu, H.-P.; Li, L.-L.; Lo, C.-F.; Lin, C.-Y.; Diau, E. W.-G. *Phys. Chem. Chem. Phys.* **2010**, *12*, 1064−1071.
(21) Rani, S.; Roy, S. C.; Paulose, M.; Varghese, O. K.; Mor, G. K.; Kim, S.; Yoriya, S.; LaTempa, T. J.; Grimes, C. A. *Phys. Chem. Chem. Phys.* **2010**, *12*, 2780−2800.
(22) Zhu, K.; Neale, N. R.; Miedaner, A.; Frank, A. J. *Nano Lett.* **2007**, *7*, 69−74.
(23) Li, L.-L.; Tsai, C.-Y.; Wu, H.-P.; Chen, C.-C.; Diau, E. W.-G. *J. Mater. Chem.* **2010**, *20*, 2753−2758.
(24) Chen, C.-C.; Say, W.-C.; Hsieh, S.-J.; Diau, E. W.-G. *Appl. Phys. A: Mater. Sci. Process* **2009**, *95*, 889−898.
(25) Chen, C.-C.; Jehng, W.-D.; Li, L.-L.; Diau, E. W.-G. *J. Electrochem. Soc.* **2009**, *156*, C304−C312.
(26) Li, L.-L.; Chen, Y.-J.; Wu, H.-P.; Wang, N.-S.; Diau, E. W.-G. *Energy Environ. Sci.* **2011**, *4*, 3420−3425.
(27) Li, L.-L.; Chang, Y.-C.; Wu, H.-P.; Diau, E. W.-G. *Int. Rev. Phys. Chem.* **2012**, *31*, 420−467.